Journal of Computational Neuroscience 19, 125–146, 2005

Dynamic Neural Network Models of the Premotoneuronal Circuitry Controlling Wrist Movements in Primates

M.A. MAIER
University Paris-6 and Paris-7 and INSERM U. 742, Université Paris-6 Pierre et Marie Curie, 9 Quai St-Bernard, 75005 Paris, France

L.E. SHUPE AND E.E. FETZ*
Department of Physiology and Biophysics and Washington National Primate Research Center, University of Washington, Seattle, WA, 98195, USA
fetz@u.washington.edu

Received June 18, 2004; Revised November 15, 2004; Accepted March 11, 2005

Action Editor: C. Carr

Abstract. Dynamic recurrent neural networks were derived to simulate neuronal populations generating bidirectional wrist movements in the monkey. The models incorporate anatomical connections of cortical and rubral neurons, muscle afferents, segmental interneurons and motoneurons; they also incorporate the response profiles of four populations of neurons observed in behaving monkeys. The networks were derived by gradient descent algorithms to generate the eight characteristic patterns of motor unit activations observed during alternating flexion-extension wrist movements. The resulting model generated the appropriate input-output transforms and developed connection strengths resembling those in physiological pathways. We found that this network could be further trained to simulate additional tasks, such as experimentally observed reflex responses to limb perturbations that stretched or shortened the active muscles, and scaling of response amplitudes in proportion to inputs. In the final comprehensive network, motor units are driven by the combined activity of cortical, rubral, spinal and afferent units during step tracking and perturbations.

The model displayed many emergent properties corresponding to physiological characteristics. The resulting neural network provides a working model of premotoneuronal circuitry and elucidates the neural mechanisms controlling motoneuron activity. It also predicts several features to be experimentally tested, for example the consequences of eliminating inhibitory connections in cortex and red nucleus. It also reveals that co-contraction can be achieved by simultaneous activation of the flexor and extensor circuits without invoking features specific to co-contraction.

Keywords: dynamic neural network, motor system, primate, wrist movement

Introduction

The neural control of limb movements in the primate has been investigated in many studies of the relation between neural activity and movement parameters (Evarts, 1981; Fetz, 1992; Georgopoulos, 1991; Porter and Lemon, 1993). More specifically, the neural circuitry controlling forelimb muscles has been elucidated by experiments on the synaptic connections and physiological discharge patterns of neurons during

*To whom correspondence should be addressed.

controlled movement tasks (Cheney et al., 1991; Fetz et al., 1989; Porter and Lemon, 1993). Of particular interest are the last-order premotoneuronal cells, found in motor cortex, red nucleus, and spinal cord. These highly interconnected regions provide the functional basis for executing motor responses. These structures are further interconnected with additional sites in cortex, cerebellum, thalamus and basal ganglia; the latter regions are not included in the current model, which focuses primarily on interactions between premotoneuronal populations.

Dynamic Recurrent Networks

Artificial neural network models can provide a causal framework for demonstrating the functional significance of physiological data. The explanatory and predictive power of these models increases with the amount of biological information they incorporate. Dynamic recurrent networks were developed to investigate the role of diverse neuronal populations during alternating flexion/extension movements of the wrist. These networks are distinguished by three properties. First, the units are dynamic, meaning that they can exhibit time-varying activity replicating the firing patterns of physiological neurons. Second, the recurrent architecture of the network allows collateral and feedback connections, which mimic anatomical pathways. Third, gradient descent learning algorithms can be used to determine the remaining free connections and activations of the network, based on examples of the behavior.

Physiological Constraints

Neural recordings in behaving monkeys have documented the physiological discharge patterns and output connections of task-related neurons at several sites involved in the control of forelimb muscles. Monkeys were trained to perform visually guided flexion and extension of the wrist. Torque generated about the wrist controlled the position of a cursor on a video monitor. The monkeys generated torques to shift the cursor into target boxes that appeared on the left or right side of the screen and maintained the cursor within the box for a variable hold period. The premotoneuronal (PreM) cells that affect muscle activity were identified by post-spike effects on their target muscles in spike-triggered averages of EMG recordings. The response patterns of three major groups of PreM cells have been documented during this task. (1) Corticomotoneuronal (CM) cells are predominantly comprised of tonic and phasic-tonic cells (Fetz and Cheney, 1980; Cheney and Fetz, 1980). Their tonic activity is proportional to the amount of static force exerted. (2) Rubromotoneuronal (RM) cells fall largely into three classes: phasic, phasic-tonic and unmodulated (Mewes, 1988; Fetz et al., 1989; Mewes and Cheney, 1994). The unmodulated cells fire throughout the task and are not related to static force. (3) Premotor dorsal root ganglion afferents exclusively fall into three categories: tonic, phasic-tonic and phasic (Flament et al., 1992). In addition, the discharge patterns of single motor units make up four classes: tonic, phasic-tonic, phasic and decrementing (Palmer and Fetz, 1985). A summary table of these response classes and their relative proportions appears in Maier et al. (1998).

Anatomical Connections

The models presented here substantially extend previous neural networks designed to simulate the wrist step-tracking task (Fetz and Shupe, 1990; Fetz et al., 1990; Fetz, 1993) and resemble a model presented previously (Maier et al., 2004). The current model comprises four modules, corresponding to cortical, rubral and segmental networks and to muscle afferents. These modules are interconnected in accordance with known anatomical pathways (Fig. 1). The cortical and rubral modules consist of excitatory projection units and local units, which are also interconnected (Fig. 2A). The segmental module consists of alpha- and gamma-motoneurons and of Ia-inhibitory interneurons. The spinal interconnections of these units (Fig. 2B) are based on anatomical and physiological data (Baldissera et al., 1981; Jankowska, 1992). The afferent module represents spindle afferent units, which are driven by gamma-motoneurons and the equivalent of applied torque, and which feed back to the segmental and supraspinal levels (Figs. 1 and 2B).

Multi-Functionality

Biological networks perform a substantial range of different behaviors. Thus realistic artificial networks should also have the ability to generate different responses. In the step-tracking task, monkeys learned to

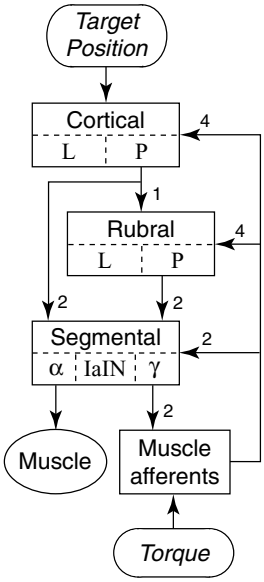

Figure 1. The network architecture comprises 4 basic unit modules: cortical, rubral and segmental units and muscle afferents. The step-tracking target position input is relayed to the cortical module, whose output units [P] project their activity to the rubral and segmental population. Both cortical and rubral units connect to the segmental level, which includes alpha- and gamma-motor units projecting to the muscle. Muscle afferents project back to the segmental and supraspinal populations. In addition, a torque feedback is given to the muscle afferents. Interactions between units of the same module involve a delay of one time step; interactions between modules usually involve longer delays, given by the number of time steps next to projection arrows.

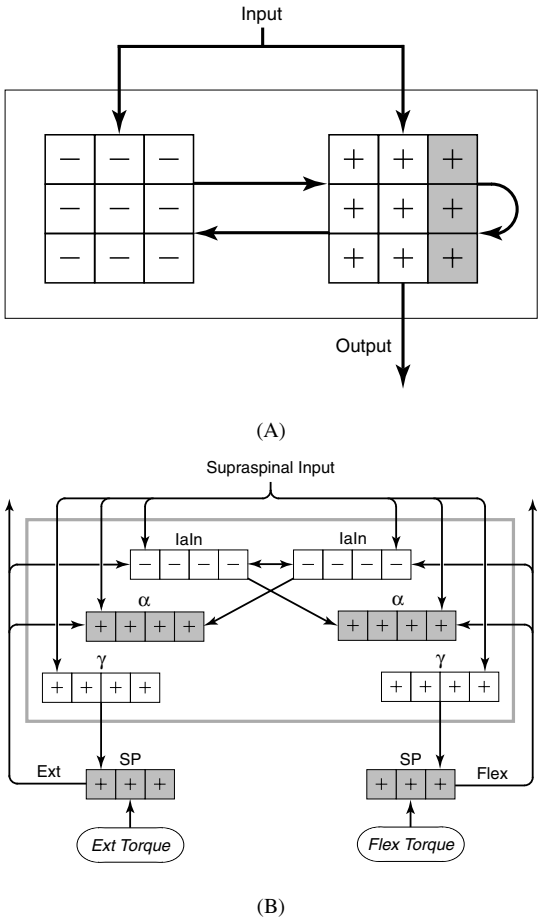

Figure 2. A: The intra-cortical and intra-rubral modules consist of equal numbers of excitatory and inhibitory units that are mutually interconnected. The excitatory units themselves are mutually interconnected (but without self-connections). Some excitatory units (shaded) have target activations corresponding to known firing patterns of CM and RM cells. The input to the supraspinal modules is distributed to both types of units, and the output arises from the excitatory units. B: The spinal cord module consists of units corresponding to alpha-motoneurons, gamma-motoneurons and Ia-inhibitory interneurons, each divided into a flexor and extensor group. The connections between these groups are modeled according to the classical stretch reflex connections. In addition, gamma-motor units drive the muscle spindle afferents (SP). Spindle afferents feed back to alpha-motor- and Ia-inhibitory units, as well as to supraspinal units. All alpha-motor units and spindle afferents (shaded) have target activation patterns. The supraspinal input to the segmental module is distributed to all units; the output consists of alpha- and gamma-motor units.

generate force levels proportional to the size of the target step. They did so by scaling the discharge rates of task-related neurons. Accordingly, the networks were trained to generate responses proportional to target sizes. Second, displacing the limb by an externally imposed perturbation evokes a segmented pattern of EMG activity: a rapid stretch of a muscle evokes a short (M1) and longer latency (M2) EMG response (Marsden et al., 1976). The EMG responses to muscle stretch and shortening perturbations, as well as the response of CM cells has been documented in the monkey during the wrist flexion/extension step-tracking task (Cheney and Fetz, 1984). Accordingly, we also trained our model to incorporate similar reflex responses. Thirdly, monkeys are able to co-contract flexor and extensor muscles in order to stiffen the wrist (Humphrey and Reed, 1983). Although the responses of CM and RM cells have not been observed under this condition, we also explored the networks' ability to generate co-contraction. Finally, we derived a comprehensive model that could emulate a repertoire of simple flexion and extension, magnitude scaling of flexion and extension and responses to external perturbations.

Methods

Training Algorithm

The network connection weights were derived using the temporal flow algorithm (Watrous and Shastri, 1986), a type of backpropagation algorithm for dynamic and recurrent networks (Williams and Zipser, 1989). This algorithm iteratively modifies the weights after each cycle to reduce the net error for generating the specified target activation patterns. Target activation patterns were obtained from the averaged firing rates of physiological neurons recorded in behaving monkeys. The net error for each target unit corresponds to the integral of the time-varying difference between the actual and the target activation. The learning rate (ε) was limited to a range of 10^{-1} to 10^{-4}. This training procedure is not intended to resemble biological learning but simply provides an effective algorithm for deriving appropriate networks that generate the required behaviors.

Topology

We will refer to elements of the artificial network as 'units' and to biological neurons as 'cells' or 'neurons'. Table 1 summarizes the constraints incorporated: the target pattern for each type of unit and the polarity and delay for every connection. We present two versions of the network model. A simpler minimally constrained 'Dual-task' model that performs two tasks: the step-tracking flexion-extension task (Maier et al., 2004) combined with one of several additional tasks and a 'comprehensive', maximally constrained model that combines four tasks.

(a) Global Organization

The four basic modules, the cortical, rubral, segmental and afferent module, are interconnected as shown in Fig. 1. The input to the network is provided by two modules: (1) the target position module conveys a representation of the target position (flexion and extension) to the cortical module, and (2) the torque feedback module provides a representation of the active torque to the afferent module. This torque feedback is represented by afferent activity since there is no explicit model of the muscles or the limb in our neural network. The connections between modules are based on anatomical and correlational evidence. Representations of the corticospinal and rubrospinal pathways provide the input to the spinal cord, and collaterals of the former connect to the red nucleus (Fromm, 1977; Humphrey et al., 1984). The muscle afferents feed back onto the spinal cord and also project to the cortical and rubral modules (via omitted cerebellar and thalamic relays). Conduction delays (Fig. 1 and Table 1) further differentiate the modules.

(b1) Internal Organization—Dual-Task Version

Input modules. The *target position* alternates between flexion and extension and is represented by a sustained step input (Fig. 5) to the network for both flexion and extension (designated as Sf and Se). Since many cells discharge dynamically to changing conditions, a brief phasic input at the onset of the target change is also provided [Df & De].

The *torque feedback* during the hold is delivered to the corresponding muscle afferents as a tonic input during flexion [Tf] and extension [Te]. Transient torque pulses, superimposed on the flexion and extension torques simulate perturbations.

Cortical module. The cortical module (Fig. 2A) consists of two kinds of *units:* local inhibitory units [CL] and spinally projecting units [CM]. This simplification of the generic cortical circuitry is intended to capture only the most essential characteristics. The *input* to cortex is distributed to both types of units (Porter et al., 1990; Fetz et al., 1991). The *output* of the cortical module consists of excitatory units that correspond to corticospinal neurons; these also have collaterals to rubral units. The intra-modular *connections* are modelled as follows: each local unit is reciprocally connected with all projection units (Baranyi et al., 1993) and projection units are mutually interconnected (Kang et al., 1988, 1991; Baranyi et al., 1993), whereas local units are not interconnected.

Rubral module. The rubral module has the same internal organization as the cortical module, but half as many units. Red Nucleus consists primarily of two types of neurons, the excitatory rubrospinal projection neuron and a local GABAergic inhibitory neuron (Nieoullon et al., 1988; Schmied et al., 1990, 1991; Mewes and Cheney, 1994). The corresponding units are abbreviated as RM and RL.

Spinal module. The spinal module consists of 3 different types of *units*, corresponding to: alpha motoneurons, gamma motoneurons and Ia-inhibitory interneurons; each set is divided into a flexor and extensor group (MUf, MUe, GMf, GMe and Iaf, Iae). The *input* from the two supraspinal modules is

Table 1. Constraints (sign, delay and strength of connection, target activation patterns) used in the basic flex/ext network and in the comprehensive network.

Basic flex—ext network		Comprehensive network	
Connection	Delay Pattern	Connection	Pattern
Input module		*Input module*	
pos e→ CMt,CM,CL	1 **tonic, phasic** {0,5}	**pos** e→ CS,CL,CE	**tonic, phasic** {0,5}
torque e→ hSP	1 **tonic** {0,4}	**torque** e→	**hSP tonic with** {0,4} **excit./inhib. burst, excit burst only.**
Cortical module		*Cortical module*	
CMt e→ CMt,CM	1 **tonic, phasic-tonic**	**CMt**,CS,CE e→ CMt,CS	**tonic, phasic-tonic, ramp, phasic-ramp with excit. burst**
CM e→ CM,CMt	1 **free**		
CMt,CM e→ CL	1	CMt,**CS** e→ CE,CL	**free**
CL i→ CMt,CM	1 **free**	**CL** i→ CMt,CS	**free**
		CE e→ CMt,CS	**free**
CMt,CM e→ RMt,RM	1	CMt,CS e→ RMt	
CMt,CM e→ RL	1	CMt,CS e→ RL	
CMt,CM e→ MN	2	CMt e→ MN	1/2a, 1/2h
CMt,CM e→ GA	2	CMt,CS e→ GA	
CMt,CM e→ IaIN	2	CMt,CS e→ IaIN	{0, 0.15}
Rubral module		*Rubral module*	
RMt,RM e→ RMt,RM	1 **tonic, phasic, phasic-tonic, bi-directional**	**RMt** e→ RM	**tonic, phasic, phasic-tonic with background activity, bidirectional**
RM,RMt e→ RL	1 **free**	RMt e→ RL	
RL i→ RMt,RM	1 **free**	RL i→ RMt	
RMt,RM e→ MN	2	RMt e→ MN	
RMt,RM e→ GA	2	RMt e→ GA	
RMt,RM e→ IaIN	2	RMt e→ IaIN	{0, 0.15}
Segmental module		*Segmental module*	
MN	**tonic, phasic, phasic-tonic, decr.**	**MN**	**tonic, phasic, phasic-tonic, decr. with M1, M2 burst**
IaIN i→ aMN	1 **free**	**IaIN** i→ aMN	**free** {-1,0}
IaIN i→ aIaIN	1	IaIN i→ aIaIN	
GA e→ hSP	2 **free** {0,3}	**GA** e→ hSP	**free** {0,3}
Afferent module		*Afferent modul*	
SP e→ hMN	2 **tonic, phasic phasic-tonic**	**SP** e→ hMN	**tonic, phasic phasic-tonic** {0.8, 5}
SP e→ hIaIN	2	SP e→ hIaIN	{2.5, 5}
SP e→ CMt,CM,CL	4	SP e→ CMt,CS,CL,CE	
SP e→ RMt,RM,RL	4	SP e→ RMt,RL	

Abbreviations: Units in **bold**: to which the target pattern (in **bold**) on the same line applies; e→: excitatory connection, range of default connection strength: $\{0, 2\}$, i→: inhibitory connection, default connection strength: $\{-2, 0\}$, a: antagonist, h: homonymous. Non-default connection strengths given in {}. For unit abbreviations, see text.

distributed to all types of units (Jankowska, 1992, Pompeiano, 1984; Clough et al., 1971). The *output* of the spinal module consists of the alpha- and gamma-motor units. The *connectivity* between the different kinds of spinal units (Fig. 2B) reflects the 'output-stage' concept (Hultborn et al., 1979), which describes the spinal control of antagonistic muscles. Each of those connections including the sign (excitatory or inhibitory) has been anatomically and physiologically described (references are given in Bullock and Contreras-Vidal, 1992, 1993). Units of a given type and group are not interconnected.

We tested the role of Renshaw cells (Windhorst, 1990) in our networks (not shown), and found that they played no critical role, as indicated by their feeble connections and non-physiological activation patterns, so they have been excluded here. Whether Renshaw cells exist in the primate cervical cord remains unclear. Data from the cat suggest their absence, at least for the extrinsic extensor muscles of the digits (Hörner et al., 1991).

Afferent module. The afferent module consists of a single type of *unit:* spindle afferents for flexion [SPf] and extension [SPe]. The *input* arises from the gamma motor units and the torque module. The excitatory *output* of the afferent module is distributed to the spinal and supraspinal modules. The afferents *connect* to the homonymous alpha motor units and the corresponding Ia-inhibitory units.

(b2) Internal Organization—Comprehensive Version

The comprehensive network consists of the Dual-task version plus the following additions.

Input modules. We further incorporate two inputs with transient torque pulses only [TFf2], [TFe2].

Cortical module. The local and the projecting units have each been subdivided: there are local inhibitory [CL] and excitatory units [CE] and there are excitatory projecting units that correspond to cortico-motoneuronal [CM] and corticospinal [CS] neurons. The *input* to the cortical module is distributed to all types cortical units except CM units and the *output* of the cortical module consists of the CM and CS units, both of which have collaterals to rubral units. Whereas CM units have connections to all spinal units including the alpha motoneurons, CS units project exclusively to spinal interneurons. The intra-modular *connections* between local and projection units are modeled as in the Dual-task version.

Rubral module. No change, except that additional input arise from CM and CS units.

Spinal module. Supraspinal input now arises from CM, CS and RM units.

Afferent module. The excitatory supraspinal *output* of the afferent module is distributed to all types of units in the cortical and rubral module.

Target Activation Patterns—Dual-Task Version

As a rule, each type of firing pattern experimentally observed in at least 20% of a neural population is represented as a single "target" unit in that population. Examples of the different types of firing patterns and their frequency during the wrist flexion-extension task are tabulated elsewhere (Fetz, 1992; Fetz et al., 1996; and references cited in the introduction). We included the phasic firing pattern of motor units, which represents at least 5% of the motor units. Firing patterns of cortical units and EMG responses during torque pulse perturbations were documented in Cheney and Fetz (1984). Table 1 lists the target patterns for each type of unit. Note that only some of the CM and RM units are provided with target patterns (namely CMt and RMt), whereas all MN and SP units have target activations. No target activations are given for CL, RL, IaIN and GA units.

Target Activation Patterns—Comprehensive Version

In order to constrain the comprehensive model as far as possible, less frequent target patterns seen in more than 5% of the population patterns were added to the cortical module such as ramp and phasic-ramp units (Table 1). Furthermore, only half of the CM units show co-contraction responses during external perturbations (Cheney and Fetz, 1984). Free CM and RM units were deleted because all representative patterns are included and all RM units have an underlying background activity.

Activation Function

The input-output function of each unit is a customized sigmoidal function, not the standard symmetric 'logistic' function (qualitatively similar networks were also obtained with the standard logistic activation function). This custom activation function describes better the input-output function of integrate-and-fire spiking

units, and facilitated the conversion of these network solutions to networks of 'spiking' units (Maier et al., 2004). The formula for this custom activation function was: $F(x) = 1/(1 + 3/x + \exp((s - x)^*T))$ where x = input, s = shift, T = temperature. The input to a unit consists of the summed activation of all other units connected to this unit times their synaptic weights.

Network Dynamics. Network units are dynamic, meaning that their activity varies over successive time steps. Thus, the changing activation of each unit represents the (normalized) firing pattern of physiologically recorded neurons. A single flexion/extension cycle (lasting about 3 s in the behavioral paradigm) was divided into 144 time steps (corresponding to a bin width or low-pass time constant of about 20 ms).

Network Initialization. Generally the weights were limited to a range of $\{0, 2\}$ for excitatory and $\{-2, 0\}$ for inhibitory units. Exceptions are given in Table 1. The networks were initialized with random connection weights distributed around an offset. This offset was positive for excitatory and negative for inhibitory units. Furthermore, this offset was positive for the position input to the cortical module and for the torque input to the afferent module.

Results

I. Minimally Constrained Basic Model

Alternating Flexion/Extension. The minimally constrained basic model and its network architecture can generate appropriate activity profiles for ramp-and-hold step-tracking movements using connection strengths resembling those in physiological pathways. The learning curve showed rapid convergence in the first 300 trials, with marginal subsequent improvements. For all tested network simulations [differing in initial randomization] the averaged errors after 1000 cycles varied between 4.1 and 4.8%; further training to 10,000 cycles reduced the average error to values between 3.5 and 3.9%. How the network achieves the input-output transformation is completely determined by the weight matrix and its associated activation patterns. A typical solution (full weight space and activation patterns) was shown in Maier et al. (2004). Here, for purpose of comparison with later dual-task models, we show a summarized weight space (Fig. 6) that indicates the principal emergent properties (typical activation patterns are shown in Fig. 4).

Figure 6 summarizes the results in terms of two or three representative units for each population: one unit active during flexion (F), one unit active during extension (E) and one bi-directional unit (B). Briefly, in the cortical module, uni-directional CM-units and target units showed preferential connections to multiple synergistic MUs activated in the same movement phase (top row). This synergistic arrangement also held for their connections to local CL units, and to RM, GA and Ia-inhibitory units. Bi-directional tonic CM units developed negligible connections to MUs. In the rubral module, in contrast, free rubral units showed bi-directional activity. The uni-directional RM target units showed essentially the same connection properties as uni-directional CM units. In the spinal module most of the Ia-inhibitory units showed uni-directional phasic-tonic activity, and inhibited the antagonist MUs and the antagonist Ia-inhibitory units. The gamma motor units [GA] develop heavy connections to the muscle spindles [SP]. The activity of the alpha motor units shows a good approximation to their four target patterns (Fig. 4). The combined input to alpha MUs consists primarily of excitatory uni-directional CM and RM units, feedback from the spindles and an inhibitory effect from the Ia-inhibitory units to assure the silence of the alpha MUs in the inactive phase. Finally, the spindles are strongly connected to the motor units [MUs] and also feed back selectively on in-phase CM, CL and RM units.

II. Minimally Constrained Dual-Task Model

Based on the simple flexion-extension model, four different dual-task models will be described: (IIa) flexion-extension with variation of the response amplitude, (IIb) flexion-extension and co-contraction, (IId) flexion-extension and response to lengthening perturbation, and (IIe) flexion-extension and response to shortening perturbation.

(IIa) Magnitude Scaling of Flexion/Extension Responses. We investigated the networks' ability to generate response amplitudes proportional to different input magnitudes. The scaling ability of the basic network trained with only one force level was tested by giving input steps of different magnitude and measuring the error between its output and the proportionally scaled target output patterns. The basic network trained at a magnitude of 1.0 and tested at input step amplitudes

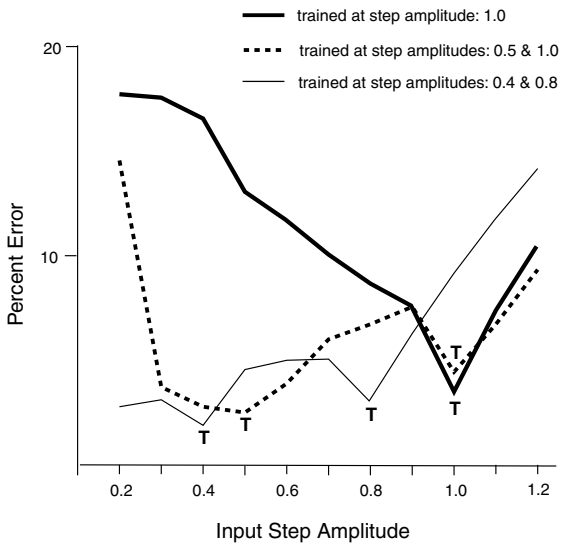

Figure 3. Error curves for different step amplitudes for three network solutions trained at specific values (T). Thick line: network trained at a single amplitude of 1.0 and tested for proportional response to other amplitudes. Stippled line: network trained at two amplitudes: 0.5 and 1.0. Thin line: network trained at amplitudes 0.4 and 0.8. Error was calculated as the difference between actual and required proportional patterns. The networks trained at two different levels show reasonable generalization over a range of amplitudes, while the network trained for a single level shows acceptable performance (<10%) in a much narrower range.

from 0.2 to 1.2 showed deviations from proportional outputs that increased with the deviation of input amplitude (Fig. 3).

Better scaling was achieved with dual-task networks trained at two input levels. One was trained at amplitudes of 0.5 and 1.0 and another at 0.4 and 0.8. Again, minimal errors occurred at the training levels. When tested with other inputs these networks show a better generalization, achieving acceptable scaling [<10% error] of target unit activity over twice the amplitude range of the basic network trained at a single level (Fig. 3).

How does the dual-task network achieve this generalization? A simple approach would be to scale the activity of all units in proportion to the input. Interestingly, this was not the case: proportional scaling was only present in some of the free CM units and almost never in the free RM units. Scaling was more pronounced in the local inhibitory CL and RL units. However, as shown in Fig. 4A, clear scaling is achieved for the target CMt and RMt units, the muscle spindles and the MUs (RMt5, the bi-directional unmodulated RM target unit, is required to not scale, in accordance with experimental observations). Furthermore, all spinal units showed clear scaling.

Since all three networks were initialized identically, their weight matrices can be directly compared: these were remarkably similar. The main differences are the weights between the free RMs and MUs, which were much smaller in the dual-task networks trained on two input steps. This may be related to the fact that the bi-directional unmodulated free RM units showed unscaled activity.

(IIb) Flexion/Extension and Co-contraction. The networks' capacity to generate co-contraction of flexor and extensor muscles in addition to reciprocal flexion/extension was investigated in a second dual-task network by giving the flexion and extension position input patterns simultaneously and requiring the simultaneous generation of the basic motor unit activation patterns. This was preceded by an alternating flexion/extension cycle (Fig. 4B). The network reached a solution with an average error of 4.3% after 10,000 training cycles. Remarkably, the solution for this co-contraction task did not require a weight matrix radically different from the solution for flexion/extension. In particular, unidirectional CM and RM units did not develop more global connections to MUs; i.e. they connected only to synergist- and not to antagonist MUs. However, the activation patterns of the non-target units showed differences between flexion/extension and co-contraction. Specifically, almost all supraspinal units (i.e. CM, CL, RM and RL) showed higher activity levels during co-contraction than during flexion/extension, without changing their overall pattern. This was probably an effect of the afferent feedback, which produced a stronger net input to all supraspinal units.

The basic networks trained to generate reciprocal flexion/extension only, when tested for co-contraction, had a threefold greater error (14%) than the dual-task network. Figure 4C shows the types of error produced: the co-contraction is incomplete and transient, since the static component of most units could not be maintained (e.g. CMt3, RMt3, SPe1, MUe1, MUe3). In contrast, networks trained to generate only co-contraction failed entirely to generate the flexion/extension cycle when tested with reciprocal inputs. Thus a network trained for flexion/extension can generate co-contraction with relatively minor changes in the weight matrix, whereas a network trained for co-contraction is utterly incompatible with alternating flexion/extension.

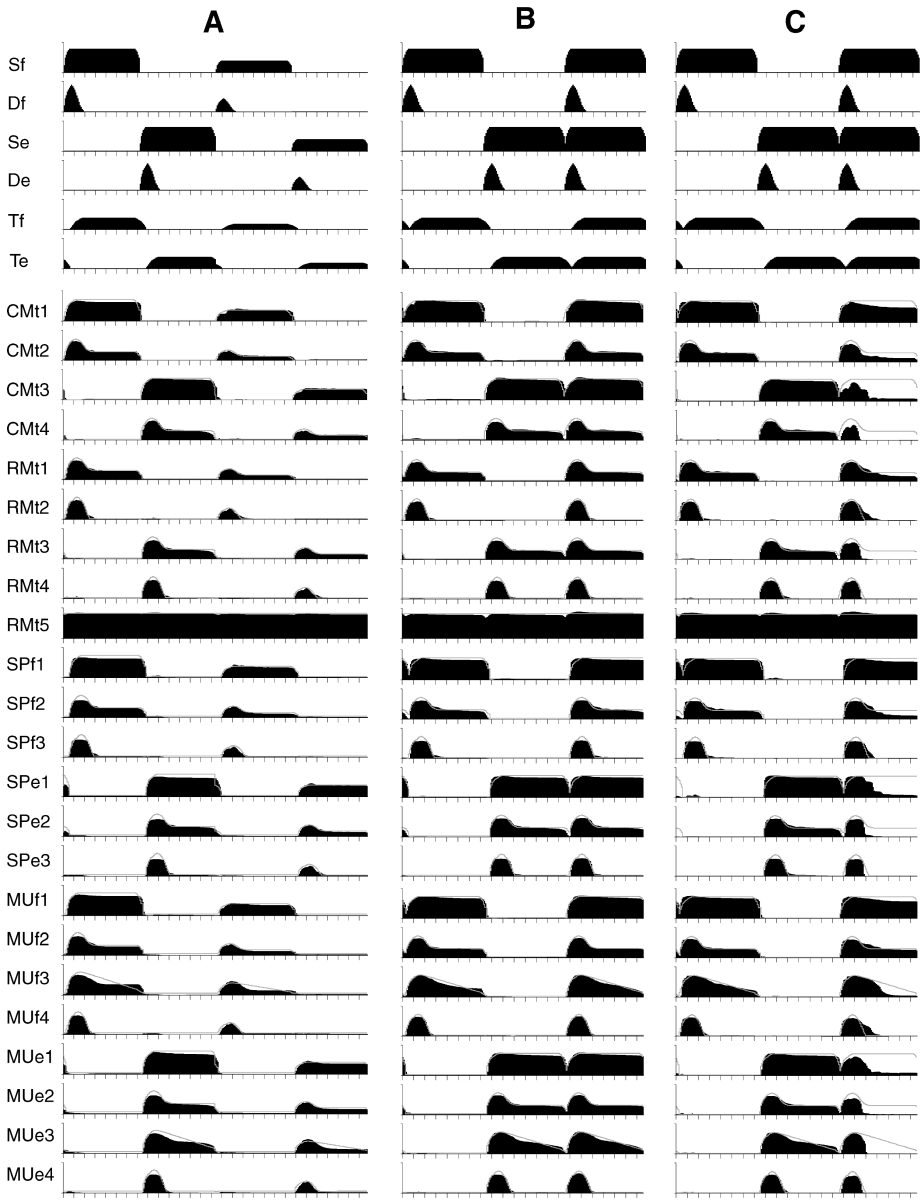

Figure 4. A: Input profiles and activation patterns for units with target activations for the network trained at two different amplitudes. A flexion/extension cycle of input amplitude 1.0 is followed by a cycle at 0.5. The target patterns are scaled accordingly. The only exception is RMt5, a non-modulated rubral target unit. Target activations (here and in Fig. 5 and 8a, 8b) were obtained from experimental data—see Methods. B: Input profiles and activation patterns for units with target activations for the network trained for flexion/extension and coactivation (averaged error 4.3%). C: Network trained purely for flexion/extension and tested for co-contraction. Dotted profiles represent appropriate activations; filled profiles give activation of the network. Deviations in the co-contraction phase are obvious for most of the units with some kind of sustained target activity (averaged error: 14%).

(IIc) Flexion/Extension and Perturbation. Reflex responses to perturbations applied to the active limb represent a fundamentally different response, which such a network could also be trained to simulate. In monkeys performing the step-tracking task, transient perturbations have been applied in two directions: stretch of the active muscles and shortening of the active muscles (Cheney and Fetz, 1984). Perturbations

which lengthened the active muscle evoked EMG responses consisting of a short-latency peak (M1) and a longer-latency peak (M2); in contrast shortening perturbations produced an initial cessation (negative M1) followed by a peak (M2). The non-active, antagonist muscle showed a brief reflex co-contraction at M2 latencies under both conditions (resulting in a transient stiffening of the wrist). Most CM cells showed an excitatory response to torque perturbations that stretched their target muscle; surprisingly, half of those also responded to shortening, usually with brief excitation. Unlike CM cells, most uni-directional RM cells showed negligible responses to torque perturbations. Spindle afferents showed a brief burst of activity when their muscle was stretched and a cessation of activity when shortened (Flament et al., 1992; Edin and Vallbo, 1990).

In a third dual-task network model these perturbations were represented by changes in the input activations of the muscle spindles; a brief torque pulse activation is delivered during each movement phase (Fig. 5 Tf and Te, see also Table 1). The target activation patterns of the spindles, CM- and RM units, as well as of the MUs reflect the experimentally observed responses to such perturbations. Everything else remains identical to the basic model so that the only source for adapting to the perturbation is the peripheral input, whose distributed effect through the network must generate the correct target responses.

(IId) Stretch Perturbation. We first tested how a basic network trained solely on the flexion/extension task would respond to the stretch perturbation. Even large stretches failed to activate the spindle afferents strongly enough to elicit any response of the MUs. When the same network was stimulated with the target activations of the spindle afferents, clear responses were elicited, but these did not correspond to the physiological pattern (Fig. 5A). Those CM units receiving afferent input showed a transient perturbation response, which they forwarded to the rubral units. Few MUs of the stretched muscle showed a clear reflex response and none of the MUs showed the antagonist M2 co-contraction burst.

When a dual-task model was trained to generate appropriate responses to the *stretch* perturbation as well as flexion/extension, its responses resembled the required activation patterns with an average error of 4.8% (Fig. 5B). The spindles show a clear transient activation during the perturbation, which is transmitted in two ways. First, this pulse is relayed to the homonymous MUs and produces an early transient response (M1). Second, the pulse is also relayed to the cortical units, and less to the RM units. The cortical response in turn produces the late phase of the homonymous response (M2) as well as the M2 response in the antagonistic MUs. This produces a brief co-contraction, which is equivalent to the stiffening response seen in the monkey.

(IIe) Shortening Perturbation. We next trained another dual-task model to respond to *shortening* perturbations of the active muscle. Figure 5C shows the responses of the units with target activations. In this case, the torque briefly drops to zero, since muscle shortening lowers the torque feedback of the spindles. Those spindles that are active during the perturbation show a corresponding decrease in activity. This response is transmitted to the homonymous MUs and appears as a transient reduction in activity (M1 off-response), followed by a brief increase (M2) produced by CM units. Similar to the stretch response, the shortening response also involves a brief increase in the antagonist muscle due to supraspinal (CM) input, producing coactivation. Certain target CM units were trained to briefly increase their activity in response to the shortening perturbation, reflecting the responses observed in primate CM cells (Cheney and Fetz, 1984).

Comparison to the Basic Network Solution. The emergent properties of the dual-task perturbation networks differed from the basic network in two ways: First, their weight space deviated from physiologically realistic solutions, exemplified by CM units that developed strong bi-directional connections. Such connections are physiologically unrealistic: CM cells involved in perturbation responses never cofacilitated flexors and extensors (Cheney and Fetz, 1984). To obtain more realistic networks we restricted the connections of the CM units to either the flexor or the extensor MU groups. The network solutions which then produced correct perturbation responses (Fig. 5B and C) are summarized in Fig. 6. Second, the network solutions to either lengthening or shortening perturbation were strikingly different from each other and thus highly task-dependent. They differed in two main aspects from solutions found for simple flexion/extension: (i) Both dual-task networks solved the task by relying less on gamma drive but more clearly on the spindle responses (torque feedback), which provide the direct and appropriate signal for generating the M1 response; (ii) in order to produce correct M2 and co-contraction responses, both

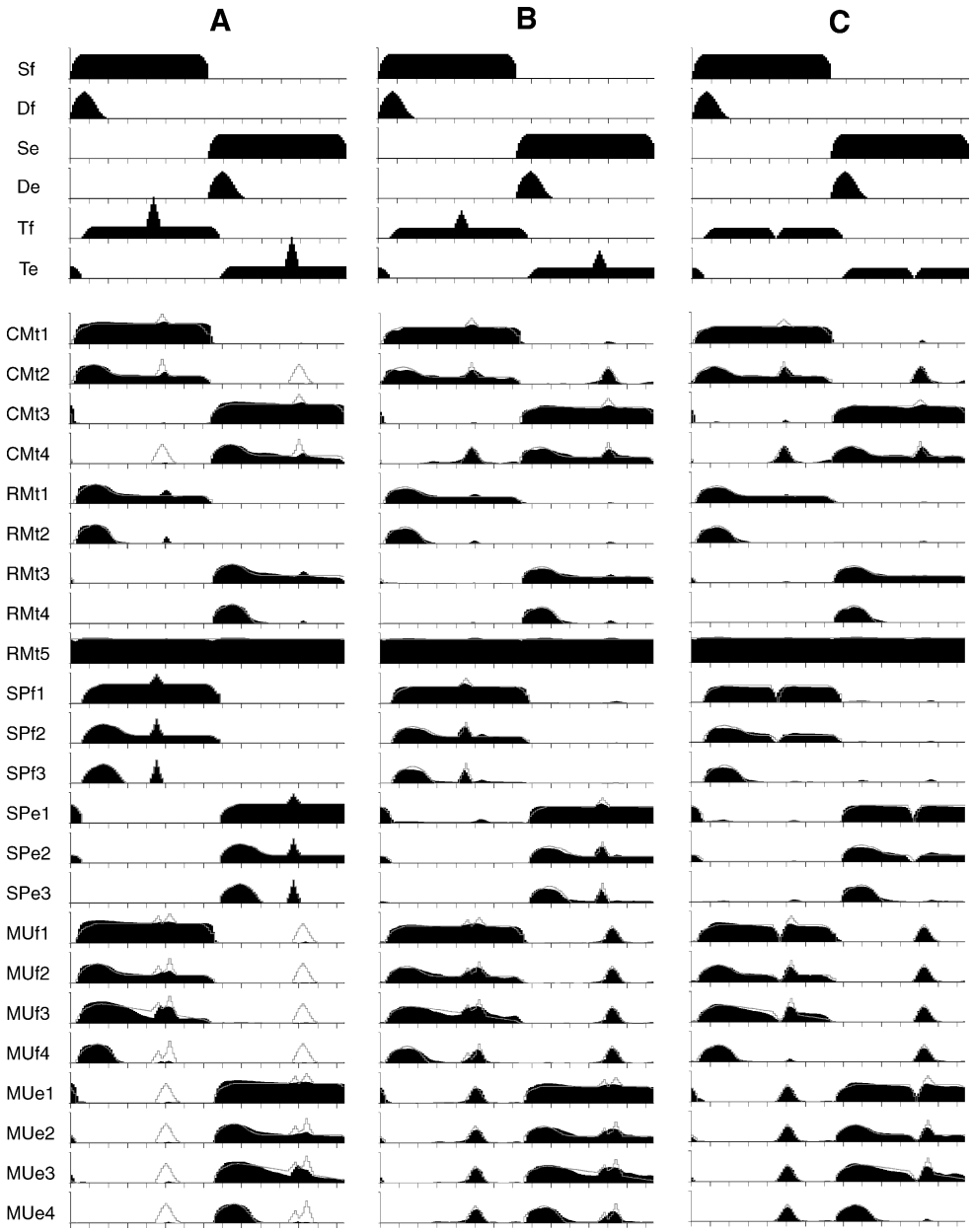

Figure 5. Network responses to proprioceptive perturbations. A: lengthening perturbations applied to the network trained only under *flexion/extension* (for 10,000 cycles). The network did not show any response to Tf and Te perturbations, so it is stimulated with the target activation patterns of the spindle afferent units [SPf1-3, SPe1-3]. This elicits transient responses in cortical and rubral units and a large combined M1 and M2 response in some of the perturbed MUs. There is, however, no co-contraction response in the antagonist MUs. Dotted profiles represent appropriate responses. B: response of a network trained to *lengthening* perturbation of the active muscle during flexion/extension. Following the perturbation (in Tf and Te), the spindles [SP] show a brief excitation which is transmitted through the network, producing brief excitation of the active motor units, and brief co-contraction in the non-active motor units. C: response of network trained to *shortening* perturbation of the active muscle during flexion/extension. The perturbation evokes a brief decrease in spindle activity, which produces a transient excitation in the cortical target units. The MUs of the active muscle show a clear inhibitory M1 response mediated by the segmental spindle feedback followed by an excitatory M2 response mediated primarily by cortical units. In addition, the MUs of the inactive muscle show a brief and late co-contraction response.

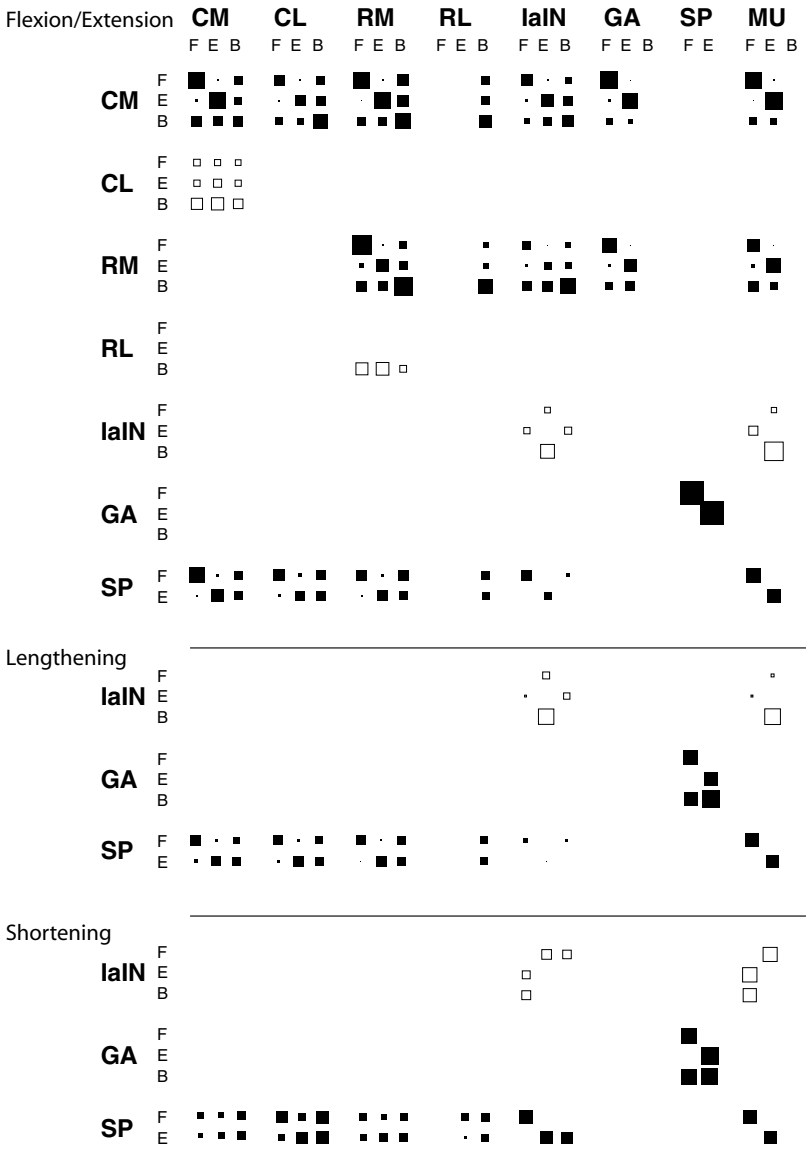

Figure 6. Schematic summary weight matrix of typical emergent connection weights for three minimally constrained "dual-task" models: *top*: simple flexion/extension, *middle*: flexion/extension and lengthening perturbation for IaIN, GA and SP units and *bottom*: flexion/extension and shortening perturbation for IaIN, GA and SP units. Activation patterns are simply classified as either being active during flexion (F), during extension (E) or during both (B). These assignments are based on the relative mean activity of original units during flexion [AF] and extension [AE]. A unit is classified as Flexion if AF/AE $>$ 1.5, Extension if AE/AF $>$ 1.5, or Both if neither inequality is satisfied. The area of the box for each comparative weight represents the average effect (mean activity $*$ connection strength) of each unit type upon another unit type. Organization of the weight space and symbols for connection strengths as in Fig. 7A, except for position and torque input units (omitted) and CS, CE (not present). Some weights are absent because one of the units did not exist. The simple flexion/extension solution shows the characteristic upper-left lower-right diagonal with moderate or strong weights indicating excitatory in-phase connections. This is true for CM, RM, GA and SP units all showing reinforcing in-phase connections between them. In contrast, the counter diagonal indicating out-of-phase connections holds for inhibitory IaINs units. This scheme of independent flexion and extension loops (except for the IaINs) is broken up when responses to perturbations are required, specifically for the afferent feedback (SP). Lengthening perturbation requires weaker in-phase connections from SP to CM and CL. Shortening requires a balance between in-phase and out-of-phase SP $->$ CL connections (in order to transform a transient inhibition response from the spindles into an excitatory perturbation response of the CM units). The IaIN and Ga units also show clear task-dependent variations of their connections strengths.

dual-task networks modified the spindle-mediated drive of CM units in such a way that CM units not only received in-phase but also out-of-phase input for generating the co-contraction burst in the antagonist MUs. However, for generating the M2 response in the agonist MUs the solutions showed task-dependent, opposite properties for the spindle-mediated in-phase input. A simple in-phase connection to the CM units provides

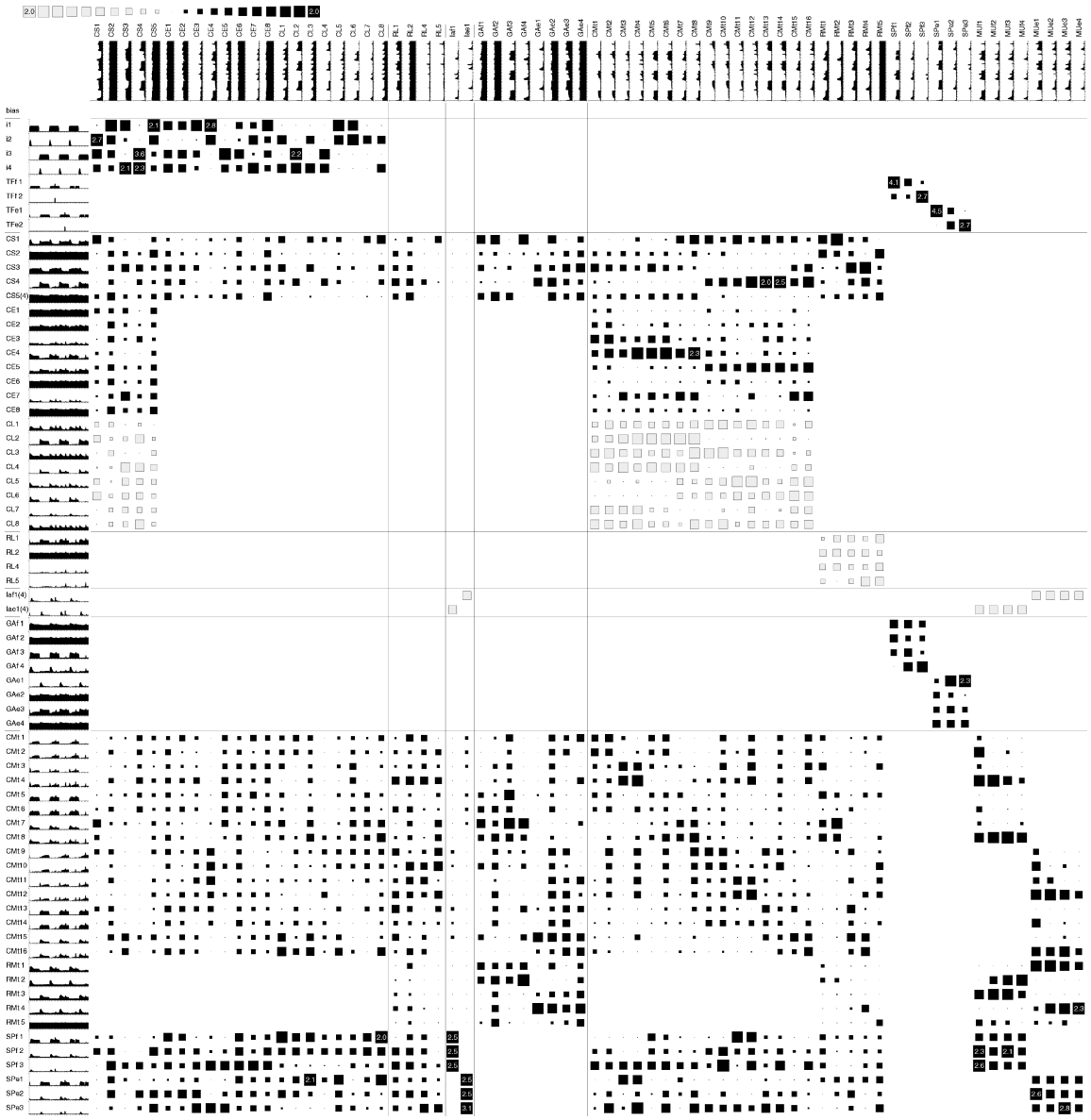

(A)

Figure 7. A: Full weight matrix for the maximally constrained comprehensive multi-task network with selected redundant units removed. Unit activations are shown at left and along the top. The connection strength from row unit to column unit is symbolized by the area of the square in the range calibrated at the top $\{-2,2\}$. Excitatory and inhibitory connections are represented by solid and open squares respectively. Numbers in parentheses after a unit's name show how many actual units (with similar activities and connections) that unit represents. Time step delays between modules are given in Fig. 1. B: Summary weight matrix for the maximally constrained comprehensive multi-task network. Same layout as Fig. 6.

(*Continued on next page.*)

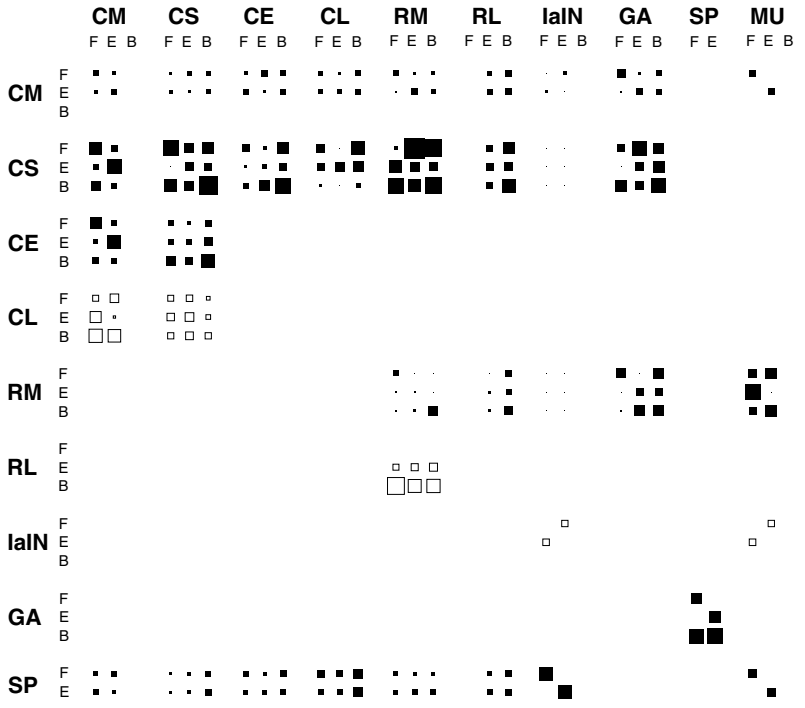

Figure 7. (*Continued*).

the excitation for the M2 burst during lengthening. In contrast, during shortening a transient inhibition must be transformed into an excitatory burst in the CM units; thus the spindles, which briefly decrease their activity, connect more strongly to the local inhibitory cortical units, which in turn produced a brief facilitation in the CM units via disinhibition.

III. Maximally Constrained Comprehensive Multi-Task Model

Ultimately, a complete model should be able to simulate all of these tasks with a single set of weights, as a trained monkey does. Obviously, for a model of this complexity our dual-task networks were not sufficiently constrained to yield physiologically compatible solutions. We therefore decided to incorporate into a comprehensive model not only all task variations simultaneously (i.e. training it to produce flexion/extension of varying amplitudes with superimposed lengthening and shortening perturbations) but also to constrain the predefined activation patterns and connection weights. The network was successively trained to perform flexion/extension without perturbation, flexion/extension with lengthening perturbation followed by flexion/extension with shortening perturbation. The magnitude of the target activation patterns varied randomly. The essential additional constraints concerned (1) the *firing patterns*: the CM target units now represent all observed firing patterns; all modulated RM target units have a background activity; free CM and RM units have been deleted and free corticospinal (non-CM) units and excitatory local cortical units have been added; and (2) the *weight space* was tuned to obtain a maximally "physiological" solution in terms of activations and connections (see Methods, Table 1). Remarkably, the network converged to a solution with an average error of approximately 5.0% after 20,000 training cycles.

The full and the summarized weight matrices are shown in Fig. 7A and B, respectively. Figure 8a shows the input and target unit activations after 20,000 training cycles: all target units show very small errors. The unified network solves the problem by using a

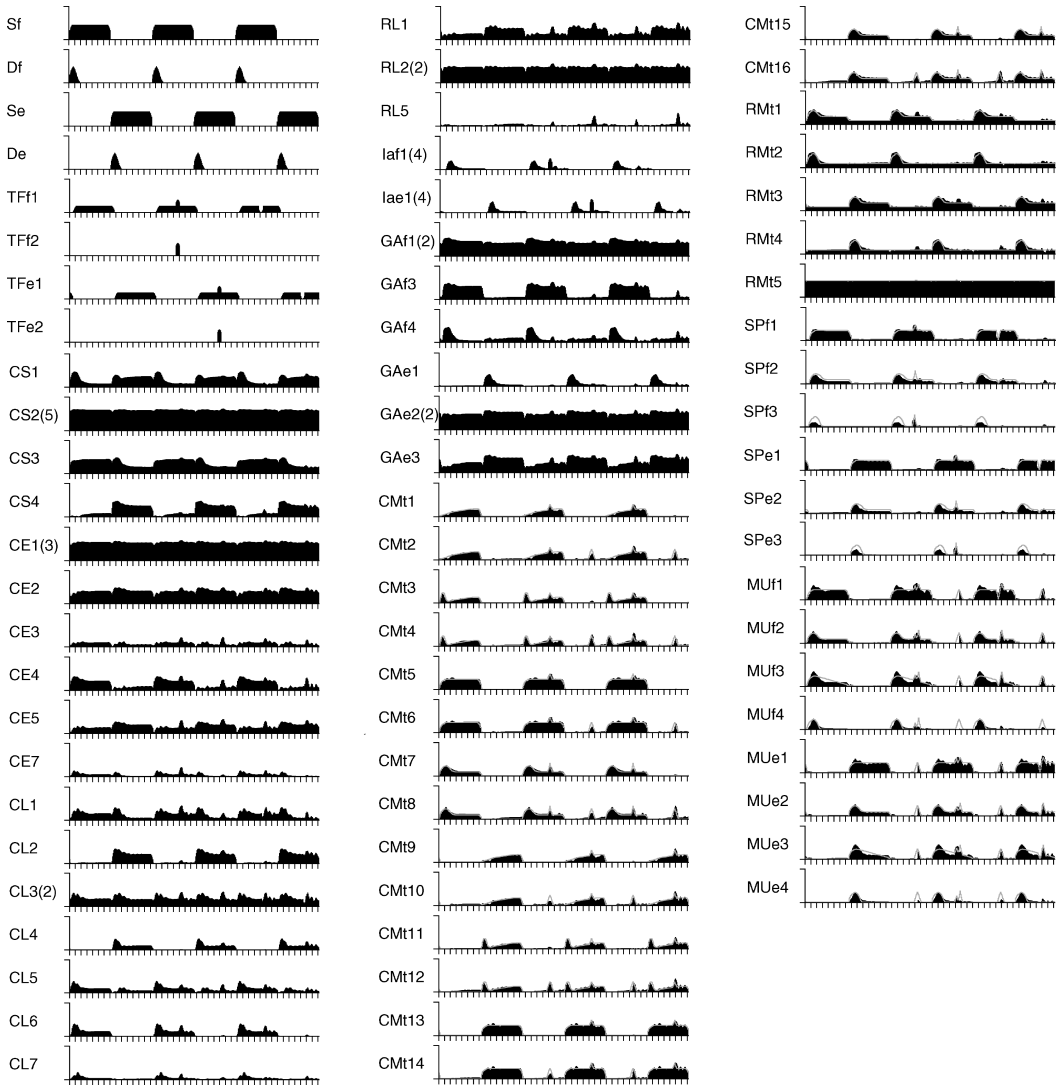

(a)

Figure 8. a: Activation patterns of units in the comprehensive multi-task network of Fig. 7A, showing a cycle of flexion/extension without perturbation, a cycle of flexion/extension with lengthening perturbation and a cycle of flexion/extension with shortening perturbation. Actual patterns of activation are shown in black and target activations shown by dotted lines. The error after 20,000 training cycles was approximately 5.0%, averaged over 1000 test cycles. Abbreviations: Sf, Df: cortical position input for flexion (static and dynamic), Se, De: same for extension, Tf, Te: torque feedback for flexion (f) and extension (e) provided to the spindle afferents, CMt: excitatory cortical projection units with cortico-motoneuronal connections and target patterns, CS: excitatory cortical projection units (non-CM), CE: excitatory local cortical units, CL: inhibitory local cortical units, RMt: excitatory rubral projection units and target patterns, RL: inhibitory local rubral units, Iaf, Iae: Ia-inhibitory units, GAf, GAe: gamma motor units, SPf, SPe: spindle afferent units, MUf, MUe: motor units. b: Responses of the comprehensive network after lesions of inhibitory cortical and rubral units. Representative units of each population in the comprehensive multi-task network are shown. Stippled lines indicate the profiles of activity in the non-lesioned network (as in Fig. 8a). A: response after lesion of a unidirectional cortical inhibitory unit CL2 . The resulting lack of cortical inhibition during the extension period produces a unidirectional increase in most units of the network including MUs, which show coactivation of flexor MUs and an overactivation of extension MUs during extension. B: response after lesion of a bidirectional cortical inhibitory unit CL3. Lack of this more general cortical inhibition produces a background increase of activity at most levels of the network and eliminates modulated activity of the flexor MUs and enhances background activity for extensor MUs, and thus leads to a generalized co-contraction. C: response after lesion of all local inhibitory rubral units (RL). This leads to only minor modifications at the cortical level but to an increase in background activity of rubral output units (RMt). This in turn produces in-phase over-activation and a loss of the temporal profile of flexor and extensor MU activity. (*Continued on next page*).

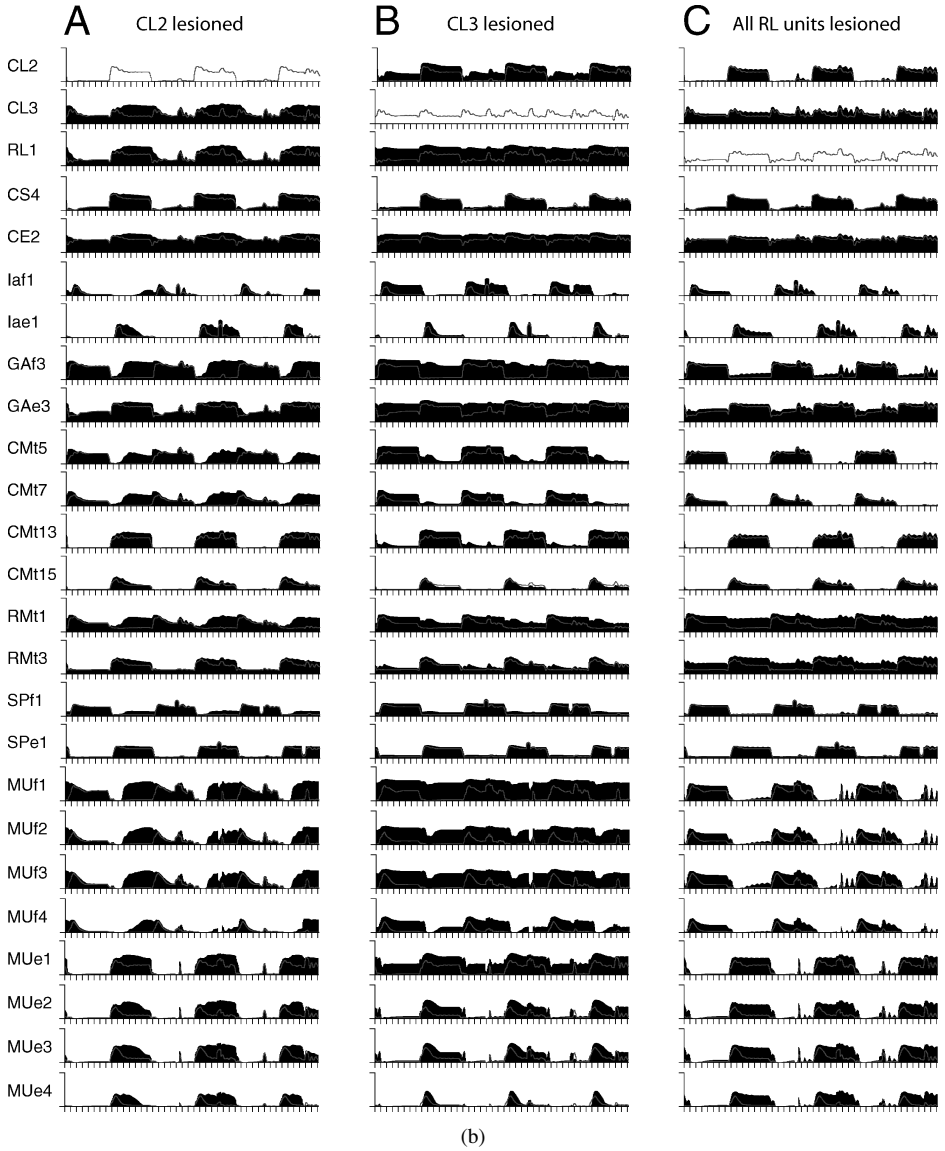

Figure 8. (*Continued*).

compromise between the lengthening and shortening solution, rather than gating; i.e. it does not dedicate particular units and connections for specific tasks. The most salient differences compared to the dual-task models concern the activation of Ia units that are driven almost exclusively by peripheral inputs from the spindle units: neither CMt nor CS units provide relevant drive to IaIN units. CS units were either tonically active and unmodulated or, like CMt units, heavily modulated in a single movement phase. Although CMt and modulated CS units excited each other in-phase, they clearly differed: CMt units more often excited in-phase rubral and spinal units, whereas CS units had less antagonistic output effects. Also, CS units showed minor responses to perturbations, whereas CMt units responded quite clearly.

IV. Responses to 'Lesions'

To obtain some predictions from the comprehensive model, its responses were tested after lesioning inhibitory cortical neurons, which would simulate the inactivation of GABAergic neurons in the primate motor

cortex. Matsumura et al. (1991, 1992) injected bicuculline, a GABA antagonist, into the primary motor cortex and observed that monkeys trying to perform a reaction-time wrist movement task co-contracted flexor and extensor muscles. This pharmacological lesion was simulated in the comprehensive model by deleting inhibitory local cortical units (CL) and testing the model's responses. Deleting all CL units totally destroyed the task modulation of the other cortical units, and consequently all of the remaining units showed unmodulated steady high activations. However, lesioning only 10% of the CL units produced more differentiated deficits. The lesion of a cortical inhibitory and *unidirectional* unit (Fig. 8b: A) produced a unidirectional increase in all CMt units (they either were overactivated or became active when they had not been). This in turn produced a unidirectional increase of activity in most units of the network including MUs, which showed unidirectional coactivation, e.g. activity of flexor MUs in extension and an overactivation (change of the temporal profile) of extension MUs during extension. This would correspond to enhanced co-contraction and increased stiffness during the on-phase of the task performance.

The lesion of a cortical inhibitory and *bidirectional* unit (Fig. 8b: B) led to a less specific lack of cortical inhibition and produced a background increase of activity at most levels of the network. This led to a loss of unidirectional activity in the flexor MUs and to enhanced background activity for the extensor MUs, and thus to a bidirectional co-contraction. This would correspond to enhanced co-contraction and increased stiffness during all phases of task performance.

Similar lesions were performed with the local inhibitory rubral units (RL). Lesion of all RL units (Fig. 8b: C) produced only minor modifications at the cortical level but led to an increase in background activity of rubral output units (RMt). This in turn produced in-phase overactivation and a loss of the temporal profiles of flexor and extensor MU activity, but had a minor impact on co-contraction.

Lesions of the Ia inhibitory units (not shown) produced minor modifications of MU activity during flexion or extension: the main effect was seen during the perturbation phase through abolishment of the inhibitory M1 response to shortening perturbation.

Discussion

Our dynamic neural network models incorporate physiological and anatomical constraints and elucidate the operation of premotoneuronal circuitry during voluntary movements. Our modeling approach differs from previous artificial neural networks that have been developed to account for other aspects of arm movement control. Focusing on cerebellar, rubral and cortical connections, Houk et al. (1993) and Berthier et al. (1993) developed a model addressing issues of motor learning and programming. Several models have concentrated on directional tuning of cortical neurons and trajectory formation during reaching (Kettner et al., 1993; Lukashin and Georgopoulos, 1993a and b; Lukashin et al., 1994, 1996a and b; Baraduc and Guigon, 2002), utilizing population coding. Other models concentrated on the cortical interaction and learning of visuomotor transformations (e.g., Guigon and Burnod, 1996; Imamizu et al., 1998; Baraduc et al., 2001). Most of these deal with vector computations rather than neuronal mechanisms. Models based on spinal circuitry were developed to simulate the dynamic behavior of muscle stretch reflex (Graham and Redman, 1993) and for control of opponent muscles during reaching (Bullock et al., 1992; Bullock and Contreras-Vidal, 1993; Bullock et al., 1994, 1998). Various analytical models deal more directly with the kinematic properties of reaching than with physiological mechanisms (e.g. Todorov and Jordan, 2002), some of these models are based on the minimum torque-change criterion (Uno et al., 1989; Kawato et al., 1990; Wada and Kawato, 1993; Gomi and Kawato, 1997), the equilibrium-point hypothesis (Massone and Bizzi, 1989; Dornay et al., 1993; Gribble et al., 1998); and adaptive controllers (Corradini et al., 1992; Hoff and Arbib, 1992).

In contrast, the present model focuses on the physiological issue of how motoneurons are synaptically controlled by various premotoneuronal structures, whose anatomy and physiology have been elucidated in the monkey and thus provide a crucial baseline for a biologically plausible model.

Constraints Used

The present neural network simulations incorporate many anatomical and physiological constraints, including the connectivity and dominant activity of major premotor populations, i.e., cortical, rubral, spinal and afferent modules, (Table 1). These constraints were incorporated by four strategies: (1) Selective and recurrent connections produce an architecture resembling the biological system. (2) Different conduction delays within and between modules provide more realistic

timing. (3) Connections can either be excitatory or inhibitory but not both. (4) Known firing patterns for most of the neurons in four populations have been introduced in the form of target activation patterns.

Correspondence to Physiological Data and Limitations of the Basic Model

The basic dual-task network model can generalize across a range of different input levels and produce appropriately scaled MU and central unit responses if it has been trained on two different levels (cf. Fetz et al., 1990). It can also incorporate reflex responses to peripheral perturbations when trained to do so. Reflex responses, scaled according to the perturbation strength, consist of several components: an initial reciprocal M1 response, followed by an M2 co-contraction of antagonist muscles.

Whereas the emergent weight space of the basic model for simple flexion/extension resembled known cortico- and rubromotoneuronal connections, that of the dual-task models including perturbation responses deviated markedly from physiological conditions: supraspinal input to MUs became predominantly bidirectional, the activity of the Ia inhibitory units was out of phase, and the solutions were heavily task-dependent. Obviously the basic model was not sufficiently constrained for finding biologically realistic solutions for the variety of tasks.

Comprehensive Model

We therefore constrained the comprehensive multi-task model more extensively by limiting the free units and by restricting the activations and the weight space to biologically plausible solutions. Independently of the initial randomization, this comprehensive network provided functional solutions: its predictive power was tested by simulating lesions of cortical inhibitory neurons, which produced responses resembling those generated by injecting bicuculline in primary motor cortex of the primate (Matsumura et al., 1991, 1992). The performance of the comprehensive multi-task model, trained to perform multiple tasks with the same set of weights, was sufficiently good to justify an analysis of its function and a comparison with physiological data.

Role of Different Group of Units

The comprehensive model suggests the functional roles that various groups of units play in these tasks. To the extent that their biological counterparts have similar activation patterns and connectivity, they could perform similar functions.

Cortical Units. CM units, all of which had target activation patterns, provided strong connections to multiple synergist MUs. This corresponds to the physiological characteristic of CM cells that produce post-spike facilitation in multiple synergistic muscles (Fetz and Cheney, 1980, 1984), and facilitate different MUs within a muscle (Mantel and Lemon, 1987). In addition to their connections to MUs, CM units also developed connections to synergistic rubral units, to Ia-inhibitory units and gamma motor units. Corresponding corticorubral and corticospinal connections have been shown to exist anatomically and physiologically (Humphrey et al., 1984; Jankowska, 1992; Clough et al., 1971).

In agreement with physiological data (Cheney and Fetz, 1984), CM units could be trained to show appropriate sensory responses to perturbations and thus to contribute significantly to producing excitatory M2 responses in both flexor and extensor MUs. CS units acquired uni- or bidirectional activations and provided excitation to rubral and spinal (Ia-inhibitory and gamma) units.

In the local cortical circuitry, uni-directional CM units tended to connect to other in-phase CM and CS units, a recurrent connection which has been described physiologically (Kang et al., 1988, 1991; Baranyi et al., 1993; Cheney and Fetz, 1985; Smith and Fetz, 1989; Porter and Lemon, 1993). Roughly half of the local inhibitory units showed bi-directional activity. Uni-directional cortical inhibitory units were connected predominantly to out-of-phase CM units, contributing to uni-directional CM activity via inhibition. Lesions of 10% of the cortical inhibitory units resulted in enhanced bidirectional CM activity, and thus in enhanced MU activation as well as muscle co-contraction, similar to effects of injection of bicuculline into motor cortex (Matsumura et al., 1991, 1992).

Rubral Units. Physiologically, more bidirectional neurons exist in the red nucleus than in the motor cortex (Mewes and Cheney, 1994) and RM cells show more co-facilitation of both flexor and extensor motoneurons

(Mewes and Cheney, 1991). The connection patterns of uni-directional rubral target units were similar to those of the unidirectional cortical projection units. Unmodulated bi-directional RM units had weaker connections to motoneurons than the uni-directional RM units, as observed physiologically (Mewes and Cheney, 1991). RM units received input primarily from CS and CM units. Lesions of all rubral units produced co-contraction, although MUs were still clearly modulated during flexion/extension; lesions of the RL units produced enhanced MU activity but no co-contraction.

Spinal Cord Units. *Ia-inhibitory interneurons* play a role in adjusting motoneuron excitability during a variety of segmental reflex activity and voluntary movements (Baldissera et al., 1981; Jankowska, 1991). In the basic model, the activation profiles as well as the connection strength of the Ia-inhibitory units were task-dependent: (Fig. 5). When responses to both types of limb perturbations were required (comprehensive model), Ia-inhibitory units developed connections consistent with physiological data, namely stronger connections between spindle afferents and the Ia-inhibitory units, as well as connections between the Ia-inhibitory units and the antagonist MUs; they also responded like afferents with a brief increase or decrease to the lengthening and shortening perturbation respectively. Their connection onto the antagonist MUs then produced either a transient decrease (through inhibition) during lengthening or a transient increase (through disinhibition) during shortening, which is functionally equivalent to the classical reciprocal inhibition in the reflex.

The function of the Ia-inhibitory units in the present model is compatible with (i) the role described by Bullock and Contreras-Vidal (1993), namely inhibiting the antagonist to prevent it from retarding agonist activity during rapid movement reversals and (ii) with the simulation of Graham and Redman (1993), in which Ia-inhibitory units prevented overshoot of the stretch reflex.

Recently, the properties of *excitatory spinal premotor-interneurons* have been described during performance of the flexion/extension task (Perlmutter et al., 1998; Maier et al., 1998) and during perturbation tasks (Prut and Perlmutter, 2003). These interneurons show no consistent relations between task-related activity and synaptic linkage to MUs and their spinal connectivity has not yet been resolved. Because of the lack of sufficiently precise constraints we chose to defer inclusion of these interneurons for future simulations.

In our model the function of the *gamma system* was limited to building up the target activation patterns of the afferents; it did so by a mixture of uni- and bidirectional and tonic non-modulated gamma motor unit activity, which was driven by supraspinal input. Without gamma drive the afferent activation patterns could not acquire phasic components, since those were not contained in the torque input.

The *spindle afferents* with imposed unidirectional target activation patterns, developed strong connections to synergistic MUs and to the Ia-inhibitory interneurons and played a crucial role during perturbations. They provided the direct signal for the M1 response in the active MUs: excitation during stretch and inhibition during shortening.

Functional Summary

The primary rationale for these simulations was to elucidate the premotoneuronal control of MUs as documented for wrist movements in behaving monkeys. The functional roles can be summarized in relation to a typical extensor MU pool and its premotor structures (a comparable situation pertains to the flexion response).

During simple and scaled flexion/extension excitatory input to MUs arrives from cortical, rubral and afferent sources, i.e. from all potential sources of the model. However, only unidirectional extension CM and RM units had strong and exclusive connections to the extensor MU pool. CM, RM, and afferent units driven in extension formed separate positive feedback loops to activate the extensor MUs. To prevent its activation by bidirectional CM and RM units during flexion, the extensor MU pool was inhibited by the antagonist (flexion) Ia-inhibitory units. This situation was demonstrated with the minimally constrained model. More complex behavior including perturbation responses was simulated with the fully constrained model.

Perturbations evoked transient bursts in MUs, with M1 and M2 components. The reciprocal M1 perturbation responses (excitatory during lengthening and inhibitory during shortening perturbations) were mediated via the afferents, which had the correct sign and latency in both cases. The M2 response, mediated by cortical excitation, involved a transient co-contraction and thus required the simultaneous activation of flexion and extension MUs. In response to extensor muscle stretch the transient excitation was transmitted from the afferents to both the extension and flexion CM units. In order to produce the counter-intuitive excitatory cortical

perturbation response of the CM units during shortening perturbations, the brief pause in afferent input was converted to excitation by the local cortical units that then disinhibited the CM units. Thus the independent excitatory loop of unidirectional CM, RM and afferent units for simple flexion/extension was deconstructed and modified with cross-connected afferent input to CM units and with inhibitory cortical cross-connections to generate appropriate responses to external perturbations.

The model makes numerous *predictions* that could be tested experimentally. First, co-contraction was achieved with a simultaneous activation of the flexor and extensor circuit usually activated reciprocally, and did not require major modifications in weights or activations to generate co-contraction. Reflex tests in humans indicate that reciprocal and co-contraction of ankle muscles involve differences in interneuronal recruitment mediated by presynaptic inhibition (Nielsen, 1998), which was not incorporated in our model. However, the prediction of the model could be experimentally tested in a monkey performing alternatively a flexion/extension and a stiffening task (Humphrey and Reed, 1983). Secondly, the role of the inhibitory cortical neurons could be further tested with bicuculline. The model predicts that during step tracking the antagonist muscles will be co-contracted due to increased activity of motor cortical output cells, as found empirically in the monkey for untrained wrist movements (Matsumura et al., 1991, 1992). Furthermore, injection of bicuculline in the red nucleus or the spinal grey matter could also be tested empirically and compared to the co-contraction patterns predicted by the model.

Acknowledgments

This work was supported in part by NIH grants NS 12542 and RR00166 and the Swiss National Science Foundation. Initial development of the recurrent neural network algorithm was supported by ONR contract N00018-89-J-1240. We thank Paul Cheney for sharing unpublished observations on the responses of RM cells.

References

Baldissera F, Hultborn H, Illert M (1981) Integration in spinal neuronal systems. In: JM Brookhart and VB Mountcastle, eds. Handbook of Physiology—the Nervous System II. American Physiological Society, Bethesda, MD.

Baraduc P, Guigon E, Burnod Y (2001) Recoding arm position to learn visuomotor transformations. Cerebral Cortex 11: 906–917.

Baraduc P, Guigon E (2002) Population computation of vectorial transformations. Neural Comput. 14: 845–871.

Baranyi A, Szente MB, Woody CD (1993) Electrophysiological characterization of different types of neurons recorded *in vivo* in the motor cortex of the cat: I. Patterns of firing activity and synaptic responses. J. Neurophysiol. 69: 1850–1864.

Berthier NE, Singh SP, Barto AG, Houk JC (1993) Distributed representation of limb motor programs in arrays of adjustable pattern generators. J. Cog. Neurosci. 5: 56–78.

Bullock D, Contreras-Vidal JL (1993) How spinal neural networks reduce discrepancies between motor intention and motor realization. In: KM Newell and DM Corcos, eds. Variability and Motor Control. Human Kinetics Press, Champaign, IL, pp. 183–221.

Bullock D, Contreras-Vidal JL, Grossberg S (1993) Equilibria and dynamics of a neural network model for opponent muscle control. In: GA Bekey and KY Goldberg, eds. Neural Networks in Robotics. Kluwer Academic Publishers, Boston/Dordrecht/London, pp. 439–457.

Bullock D, Grossberg S (1992) Emergence of tri-phasic muscle activation from the nonlinear interactions of central and spinal neural network circuits. Human Movement Sci. 11: 157–167.

Bullock D, Grossberg S, Guenther FH (1993) A self-organizing neural model of motor equivalent reaching and tool use by a multijoint arm. J. Cog. Neurosci. 5: 408–435.

Bullock D, Cisek P, Grossberg S (1998) Cortical networks for control of voluntary arm movements under variable force conditions. Cerebral Cortex 8: 48–62.

Buys EJ, Lemon RN, Mantel GWH, Muir RB (1986) Selective facilitation of different hand muscles by single corticospinal neurones in the conscious monkey. J. Physiol. 381: 529–549.

Cheney PD, Fetz EE (1980) Functional classes of primate corticomotoneural cells and their relation to active force. J. Neurophysiol. 44: 773–791.

Cheney PD, Fetz EE (1984) Corticomotoneuronal cells contribute to long-latency stretch reflexes in the Rhesus monkey. J. Physiol. 349: 249–272.

Cheney PD, Fetz EE (1985) Comparable patterns of muscle facilitation evoked by individual corticomotoneuronal (CM) cells and by single intracortical microstimuli in primates: Evidence for functional groups of CM cells. J. Neurophysiol. 53: 786–804.

Cheney PD, Fetz EE, Mewes K (1991) Neural mechanisms underlying corticospinal and rubrospinal control of limb movements. Prog. Brain Res. 87: 213–252.

Clough JFM, Phillips CG, Sheridan JD (1971) The short-latency projection from the baboons' motor cortex to fusimotor neurones of the forearm and hand. J. Physiol. 216: 257–279.

Corradini ML, Gentilucci M, Leo T, Rizzolatti G (1992) Motor control of voluntary arm movements. Kinematic and modelling study. Biological Cybernetics 67: 347–360.

Dornay M, Mussa-Ivaldi FA, McIntyre J, Bizzi E (1993) Stability constraints for the distributed control of motor behavior. Neural Networks 6: 1045–1059.

Evarts EV (1981) Role of motor cortex in voluntary movements in primates. In: JM Brookhart, VB Mountcastle, eds. Handbook of Physiology—The Nervous System II. American Physiological Society, Bethesda, Maryland, pp. 1083–1120.

Edin BB, Vallbo AB (1990) Dynamic response of human muscle spindle afferents to stretch. J. Neurophysiol. 63: 1297–1306.

Fetz EE (1992) Are movement parameters recognizably coded in the activity of single neurons? Behav. Brain Sci. 15: 679–690.

Fetz EE (1993) Dynamic recurrent neural network models of sensorimotor behavior. In: D Gardner, ed. The Neurobiology of Neural Networks. MIT Press, Cambridge MA. pp. 165–190.

Fetz EE, Cheney PD (1980) Postspike facilitation of forelimb muscle activity by primate corticomotoneuronal cells. J. Neurophysiol. 44: 751–772.

Fetz EE, Cheney PD, Mewes K, Palmer S (1989) Control of forelimb muscle activity by populations of corticomotoneuronal and rubromotoneuronal cells. Prog. Brain Res. 80: 437–449.

Fetz EE, Shupe LE (1990) Neural network models of the primate motor system. In: R Eckmiller, ed. Advanced Neural Computers. Elsevier Science Publishers B.V., North-Holland, pp. 43–50.

Fetz EE, Shupe LE, Murthy VN (1990) Neural networks controlling wrist movement. PIJCNN 2: 675–679.

Fetz EE, Toyama K, Smith WS (1991) Synaptic interactions between cortical neurons. In: A Peters, EG Joness, eds. Cerebral Cortex, Vol IX. Plenum Publishing Corporation. pp. 1–47.

Fetz EE, Perlmutter SI, Maier MA, Flament D, Fortier PA (1996) Response patterns and post-spike effects of premotor neurons in cervical spinal cord of behaving monkeys. Can. J. Physiol. and Pharm. 74: 531–546.

Flament D, Fortier PA, Fetz EE (1992) Response patterns and post-spike effects of peripheral afferents in dorsal root ganglia of behaving monkeys. J. Neurophysiol. 67: 875–889.

Fromm C (1983) Contrasting properties of pyramidal tract neurons located in the precentral or postcentral areas and of corticorubral neurons in the behaving monkey. Adv. Neurol. 39: 329–345.

Georgopoulos AP (1991) Higher order motor control. Annual Review of Neuroscience 14: 361–377.

Gomi H, Kawato M (1997) Human arm stiffness and equilibrium-point trajectory during multi-joint movement. Biolological Cybernetics 76: 163–171.

Graham BP, Redman SJ (1993) Dynamic behavior of a model of the muscle stretch reflex. Neural Net. 6: 947–962.

Gribble PL, Ostry DJ, Sanguineti V, Laboissière R (1998) Are complex control signals required for human arm movement? J. Neurophysiol. 79: 1409–24.

Guigon E, Burnod Y (1995) Modelling the acquisition of goal-directed behaviors by population of neurons. Int. J. Psychophysiol. 19: 103–113.

Hoff B, Arbib MA (1992) A model of the effects of speed, accuracy, and perturbation of visually guided reaching. In: R Caminiti, P Johnson, Y Burnod, eds. Control of Arm Movement in Space: Neurophysiological and Computational Approaches. Springer, Berlin, New York. pp. 285–306.

Hörner M, Illert M, Kümmel H (1991) Absence of recurrent axon collaterals in motoneurones to the extrinsic digit extensor muscles of the cat forelimb. Neurosci. Let. 122: 183–186.

Houk JC, Keifer J, Barto AG (1993) Distributed motor commands in the limb premotor network. Trends Neurosci. 16: 27–33.

Hultborn H, Jankowska H, Lindstrom S (1971) Recurrent inhibition of interneurons monosynaptically activated from group Ia afferents. J. Physiol. 215: 613–636.

Hultborn H, Lindstrom S, Wigstrom H (1979) On the function of recurrent inhibition in the spinal cord. Exp. Brain Res. 37: 399–403.

Humphrey DR, Reed DJ (1983) Separate cortical systems for control of joint movement and joint stiffness: reciprocal activation and coactivation of antagonist muscles. In: JE Desmedt, ed. Motor Control Mechanisms in Health and Disease: Advances in Neurology 39. Raven Press, New York, pp. 347–372.

Humphrey DR, Gold R, Reed DJ (1984) Sizes, laminar and topographic origins of cortical projections to the major divisions of the red nucleus in the monkey. J. Comp. Neurol. 225: 75–94.

Imamizu H, Uno Y, Kawato M (1998) Adaptive internal model of intrinsic kinematics involved in learning an aiming task. J. Exp. Psychol. and Human Perceptual Performance 3: 812–829.

Jankowska E (1992) Interneuronal relay in spinal pathways from proprioceptors. Prog. Neurobiol. 38: 335–378.

Kang Y, Endo K, Araki T (1988) Excitarory synaptic actions between pairs of neighboring pyramidal tract cells in the motor cortex. J. Neurophysiol. 59: 636–647.

Kang Y, Endo K, Araki T (1991) Differential connections by intracortical axon collaterals among pyramidal tract cells in the cat motor cortex. J. Physiol. 435: 243–256.

Kawato M, Maeda Y, Uno Y, Suzuki R (1990) Trajectory formation of arm movement by cascade neural network model based on minimum torque-change criterion. Biological Cybernetics 62: 275–288.

Kettner R, Marcario J, Port N (1993) A neural network model of ortical activity during reaching. J. Cog. Neurosci. 5: 14–33.

Lukashin AV, Georgopoulos AP (1993) A dynamical neural network model for motor cortical activity during movement: population coding of movement trajectories. Biological Cybernetics 69: 517–524.

Lukashin AV, Wilcox GL, Georgopoulos AP (1994) Overlapping neural networks for multiple motor engrams. Proc. Natl. Acad. Sci. 91: 8651–8654.

Lukashin AV, Amirikian BR, Georgopoulos AP (1996) A simulated actuator driven by motor cortical signals. NeuroReport 7: 2597–2601.

Lukashin AV, Wilcox GL, Georgopoulos AP (1996) Modeling of directional operations in the motor cortex: a noisy network of spiking neurons is trained to generate a neural-vector trajectory. Neural Net. 9: 937–410.

Maier MA, Shupe LE, Fetz EE (2004) Recurrent neural networks of integrate-and-fire cells simulating short-term memory and wrist movement tasks derived from continuous dynamic networks. J. Physiol. (Paris) 97: 601–612.

Maier MA, Perlmutter SI, Fetz EE (1998) Response patterns and force relations of monkey spinal interneurons during active wrist movement. J. Neurophysiol. 80: 2495–2513.

Mantel GWH, Lemon RN (1987) Cross-correlation reveals facilitation of single motor units in thenar muscles by single corticospinal neurones in the conscious monkey. Neurosci. Let. 77: 113–118.

Marsden CD, Merton PA, Morton HB (1976) Stretch reflex and servo action in a variety of human muscles. J. Physiol. 259: 531–560.

Massone L, Bizzi E (1989) A neural network model for limb trajectory formation. Biological Cybernetics 61: 417–425.

Matsumura M, Sawaguchi T, Oishi T, Ueki K, Kubota K (1991) Behavioral deficits induced by local injection of bicuculline and muscimol into the primate motor and premotor cortex. J. Neurophysiol. 65: 1542–1553.

Matsumura M, Sawaguchi T, Kubota K (1992) GABAergic inhibition of neuronal activity in the primate motor and premotor cortex during voluntary movement. J. Neurophysiol. 68: 692–702.

Mewes K, Cheney PD (1994) Primate rubromotoneuronal cells: parametric relations and contribution to wrist movement. J. Neurophysiol. 72: 14–30.

Nielsen JB (1998) Co-contraction of antagonistic muscles in man. Danish Medical Bulletin, 45: 423–435.

Nieoullon A, Vuillon-Cacciuttolo G, Dusticier N, Kerkerian L, Andre D, Bosler O (1988) Putative neurotransmitters in the red nucleus and their involvement in postlesion adaptive mechanisms. Behav. Brain Res. 28: 163–174.

Palmer SS, Fetz EE (1985) Discharge proprties of primate forearm motor units during isometric muscle activity. J. Neurophysiol. 54: 1178–1193.

Perlmutter SI, Maier MA, Fetz EE (1998) Activity of spinal interneurons their effects on forearm muscles during voluntary wrist movements in the monkey. J. Neurophysiol. 80: 2475–2494.

Pompeiano O (1984) Recurrent inhibition. In: RA Davidoff, ed. Handbook of the Spinal Cord. Marcel Dekker, New York. pp. 461–557.

Porter LL, Sakamoto T, Asanuma H (1990) Morphological and physiological identification of neurons in the cat motor cortex which receive direct input from the somatic sensory cortex. Exp. Brain Res. 80: 209–212.

Porter R, Lemon RN (1993) Corticospinal Functiona and Voluntary Movement. Oxford University Press, Oxford.

Prut Y, Perlmutter SI (2003) Firing properties of spinal interneurons during voluntary movement. I. State-dependent regularity of firing. J. Neurosci. 23: 9600–9610.

Schmied A, Amalric M, Dormont JF, Farin D (1991) GABAergic control of rubral single unit activity during a reaction time task. Exp. Brain Res. 84: 285–296.

Schmied A, Farin D, Amalric M, Dormont JF (1991) Changes in motor performance and rubral single unit activity in cats after microinjections of serotonin into the red nucleus area. Brain Res. 567: 91–100.

Tatton WG, Bawa P (1979) Input-output properties of motor unit responses in muscles stretched by imposed displacements of the monkey wrist. Exp Brain Res. 37: 439–457.

Todorov E, Jordan MI (2002) Optimal feedback control as a theory of motor coordination. Nature Neurosci. 5: 1226–35.

Uno Y, Kawato M, Suzuki R (1989) Formation and control of optimal trajectory in human multijoint arm movements. Biological Cybernetics 61: 89–101.

Wada Y, Kawato M (1993) A neural network model for arm trajectory formation using forward and inverse dynamics models. Neural Net. 6: 919–932.

Watrous RL, Shastri L (1986) Learning phonetic features using connectionist networks: an experiment in speech recognition. Technical Report MS-CIS-86-78, Linc Lab 44, University of Pensylvania.

Williams RJ, Zipser D (1989) A learning algorithm for continually running fully recurrent neural networks. Neural Comp. 1: 270–280.

Windhorst U (1990) Activation of renshaw cells. Prog. Neurobiol. 35: 135–179.